Available online at www.sciencedirect.com
ScienceDirect
C. R. Mecanique 337 (2009) 61–67
COMPTES RENDUS MECANIQUE

Vortex identification and tracking in unsteady flows

Arganthaël Berson [a,*], Marc Michard [b], Philippe Blanc-Benon [b]

[a] *Fuel Cell Research Centre, Queen's University, 945, Princess St., Kingston ON, K7L 5L9, Canada*
[b] *LMFA UMR CNRS 5509, École centrale de Lyon, 36, avenue Guy-de-Collongue, 69134 Ecully Cedex, France*

Received 14 November 2008; accepted after revision 2 March 2009

Presented by Geneviève Comte-Bellot

Abstract

The present Note deals with the identification and tracking of vortices in a time-resolved unsteady flow. The approach is based on the combination of two existing post-processing tools that are Galilean invariant functions: feature flow field $\boldsymbol{f}$ and vortex identification algorithm γ_2. An analytical development shows that the joint use of γ_2 and the streamlines of $\boldsymbol{f}$ allows to identify and track the location of the center of a vortex core with a non-zero convection velocity. We discuss the applicability of this procedure to actual flows for which the assumptions of the analytical approach may not be strictly valid. The procedure is validated using PIV measurements performed in an oscillating flow in a model of thermoacoustic refrigerator. This method proves to be efficient for the automated analysis of convection processes when large numbers of vortices are involved. ***To cite this article: A. Berson et al., C. R. Mecanique 337 (2009).***

Keywords: Fluid mechanics; Vortex tracking; Feature flow field; Unsteady flow; PIV

1. Introduction

The tracking of some remarkable points, such as critical points, remains an important issue when dealing with unsteady flows (oscillating flows, instabilities in shear layers, flow separation) [1–3]. According to Chong et al. [1], *critical points are points in the flow where all three velocity components are zero and the streamline slope is indeterminate*. For example, the center of a vortex core with zero velocity is a critical point (node point). However, in most practical applications, critical points of interest in the flow domain are advected, i.e. they have non-zero velocity components. Moreover, due to the large amount of experimental data (e.g. provided by phase-locked PIV in periodic flows, or time-resolved PIV in rapidly changing flows), it is necessary to track the locations of vortices with automated procedures. The present paper focuses on the study of time-resolved flows including a large number of vortices advected with non-zero velocities. For that purpose, we study the link between two different post-processing tools:

* Corresponding author.
E-mail addresses: berson@queensu.ca (A. Berson), marc.michard@ec-lyon.fr (M. Michard), philippe.blanc-benon@ec-lyon.fr (Ph. Blanc-Benon).

1631-0721/$ – see front matter
doi:10.1016/j.crme.2009.03.006

– the first one is named feature flow field $\boldsymbol{f}$ and has been previously used for the tracking of critical points in a two-dimensional flow;
– the second one, the so-called γ_2 function, is used for the identification of vortical structures in two-dimensional flows.

In Section 2, we investigate the case of a two-dimensional time-dependent velocity field using an analytical derivation. In Section 3, the applicability of the method is demonstrated using actual PIV measurements in an unsteady flow. Conclusions are given in Section 4.

2. Theoretical developments

2.1. Feature flow field and tracking of critical points

For the tracking of critical points in a time-dependent velocity field, the concept of feature flow field as introduced by Theisel and Seidel [4] is very useful. Given a two-dimensional velocity field $\boldsymbol{u}(x, y, t)$, these authors define a three-dimensional vector $\boldsymbol{f}(x, y, t)$ as:

$$\boldsymbol{f}(x, y, t) = \text{grad}(u) \times \text{grad}(v) \tag{1}$$

where u and v are velocity components in the (x, y) plane and the $\times$ operator refers here to a vector product. As the velocity field varies with time, $\boldsymbol{f}(x, y, t)$ is defined so that it points towards the direction of minimal change for both velocity components. This direction is given by the intersection of the planes perpendicular to the gradients of each velocity components, in a first-order approximation. Thus, the streamlines of $\boldsymbol{f}$ integrated from a given critical point of $\boldsymbol{u}$ define the trajectory and behavior of this point in time. For this reason, $\boldsymbol{f}$ is called feature flow field (hereafter denoted FFF) of $\boldsymbol{u}$. Eq. (1) can be rewritten in a more practical form as:

$$\boldsymbol{f}(x, y, t) = (u_y v_t - u_t v_y,\ u_t v_x - u_x v_t,\ u_x v_y - u_y v_x)^T \tag{2}$$

where x, y and t subscripts denote partial derivatives with respect to these variables, T superscript is the transpose. Note that FFF requires a velocity field that is continuous in time. Practically, given two velocity fields $\boldsymbol{u_0}(x, y)$ and $\boldsymbol{u_1}(x, y)$, which are, for instance, extracted from PIV measurements at two successive discrete time steps t_0 and t_1, Theisel and Seidel [4] compute $\boldsymbol{f}$ in Eq. (2) from an interpolated time-dependent velocity field $\boldsymbol{u}(x, y, t)$ given at any time t between $t_0 = 0$ and $t_1 = 1$ by:

$$\boldsymbol{u}(x, y, t) = (1 - t)\boldsymbol{u_0}(x, y) + t\boldsymbol{u_1}(x, y) \tag{3}$$

The streamlines of $\boldsymbol{f}$ describe the trajectory of critical points in the three-dimensional space (x, y, t). Depardon et al. [3] apply this procedure to the study of flow separation around a wall-mounted cube. In a first step, these authors identify critical points of three types at t_0 and t_1 using three scalar functions: Γ_1 (initially defined by Graftieaux et al. [5]) for a node point, K_1 (which is a modified version of the definition of Γ_1) for a focus point and G_1 for a saddle point. In a second step, the authors associate the location of the critical points at t_0 and t_1 using streamlines of $\boldsymbol{f}$.

2.2. Identification of vortex cores: Γ_2 and γ_2 functions

When dealing with the identification of vortex cores, the main drawback of the approach of Depardon et al. [3] is that scalar functions like Γ_1 are not Galilean invariant: Γ_1 fails to identify the location of the center of a vortex that is convected with a large velocity, whereas it is correctly identified in a reference frame moving with this convection velocity. To overcome this difficulty, Favelier et al. [6] proposed a modified definition of Γ_1. This new function, called Γ_2, is defined at any location $\boldsymbol{x}$ inside the flow domain (Fig. 1) by:

$$\Gamma_2(\boldsymbol{x}) = \frac{1}{S} \oint_{\boldsymbol{x'} \in S} \sin(\theta)\, \mathrm{d}x'_1\, \mathrm{d}x'_2 \tag{4}$$

where S is a circle with center $\boldsymbol{x}$ and θ denotes the angle between $\boldsymbol{x'} - \boldsymbol{x}$ and the relative velocity $\boldsymbol{u}(\boldsymbol{x'}) - \boldsymbol{u}(\boldsymbol{x})$ in a reference frame moving with the local velocity $\boldsymbol{u}(\boldsymbol{x})$. The radius R of the circle is an adjustable parameter, which is

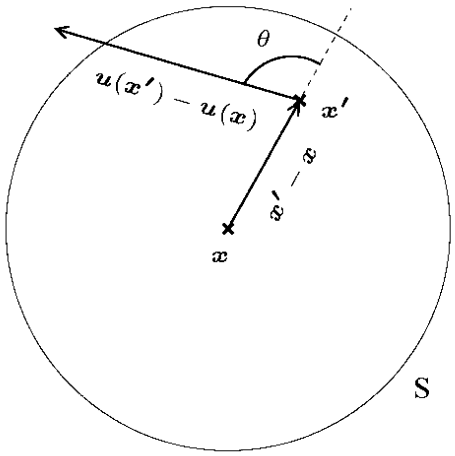

Fig. 1. Definition of angle θ for Γ_2.

chosen according to the characteristic length of the vortices and the size of the PIV mesh grid. However, Favelier et al. [6] demonstrated that Γ_2 varies very slowly with R and in practice R is chosen as twice the size of the PIV mesh grid. With this definition, it is clear that Γ_2 is Galilean invariant, dimensionless and ranging between -1 and 1. It is a top-hat function reaching its maximum value at the center of a vortex, and with large gradients at the boundary of the vortex. Assuming that the radius R is small, Favelier et al. [6] used a first-order Taylor expansion of the velocity field around $\boldsymbol{x}$. They found that Γ_2 tends towards a local function called γ_2, which is independent of the initial arbitrary choice of R, given by:

$$\gamma_2(\boldsymbol{x}) = \frac{\operatorname{sign}(\omega)}{\pi}\left\{\left(1-|\mu|\right)F\left[\frac{2\sqrt{|\mu|}}{1+|\mu|}\right] + \left(1+|\mu|\right)E\left[\frac{2\sqrt{|\mu|}}{1+|\mu|}\right]\right\} \tag{5}$$

In Eq. (5), F and E denote the complete elliptic integrals of the first and second order respectively and $\mu = \lambda/\omega$ is the ratio between the local straining rate λ and rotation rate ω in the principal axes of the straining rate tensor at $\boldsymbol{x}$.

For two-dimensional incompressible flows, the inner core of a vortex is usually defined by the condition $\omega^2 - \lambda^2 \geqslant 0$ (see for example the popular criteria λ_2 (Jeong and Hussain [7]) or Q (Hunt et al. [8], Chong et al. [1])). It can be shown that this condition is strictly equivalent to $|\gamma_2| \geqslant 2/\pi$. Therefore, the boundary of a vortex is a closed curve along which $|\gamma_2| = 2/\pi$.

2.3. Relation between γ_2 and feature flow field

In the present work, we address two problems that are not clear in the literature:

- when do streamlines of $\boldsymbol{f}$ go forward or backward in time?
- can any point located inside a vortex core with a non-zero convection velocity be tracked with FFF?

For the sake of simplicity, we assume that $t_0 = 0$ and $t_1 = 1$. We consider a point $\boldsymbol{x} = (x, y)$ where the fluid velocity is $\boldsymbol{u} = (u, v)$. The fluid velocity at time t_0 and at any location $\boldsymbol{x'} = (x', y')$ in the vicinity of $\boldsymbol{x}$ is given by a first-order Taylor expansion:

$$\begin{pmatrix} u_0(x', y') \\ v_0(x', y') \end{pmatrix} = \begin{pmatrix} u - \lambda(x'-x) + \omega(y'-y) \\ v - \omega(x'-x) + \lambda(y'-y) \end{pmatrix} \tag{6}$$

We investigate the pattern of the streamlines of $\boldsymbol{f}$ originating at t_0 from points $\boldsymbol{x'}$, for the specific case where $\boldsymbol{u_1}$ is a translation of $\boldsymbol{u_0}$ by a given spatial shift x_0 along direction x (pure advection):

$$\boldsymbol{u_1}(x', y') = \boldsymbol{u_0}(x' - x_0, y') \tag{7}$$

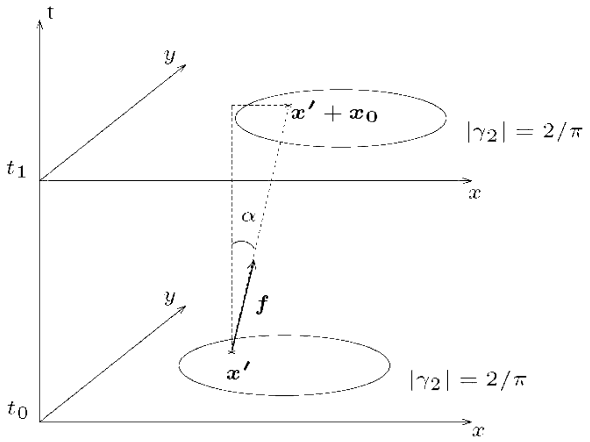

Fig. 2. Streamlines of $\boldsymbol{f}$ for an arbitrary small advection of a vortex: if $\boldsymbol{x'}$ is located inside a vortex core ($2/\pi < |\gamma_2| < 1$), the streamline is a straight line that relates exactly the original location of $\boldsymbol{x'}$ at t_0 to its new location at t_1.

The Taylor expansion of the velocity field at t_1 gives:

$$\begin{pmatrix} u_1(x', y') \\ v_1(x', y') \end{pmatrix} = \begin{pmatrix} u - \lambda(x' - x_0 - x) + \omega(y' - y) \\ v - \omega(x' - x_0 - x) + \lambda(y' - y) \end{pmatrix} \tag{8}$$

which implicitly assumes that the spatial shift x_0 is much smaller than the characteristic length scale of the vortex core.

Combining Eqs. (2), (3), (6) and (8) straightforwardly leads to the expression of $\boldsymbol{f}(x', y', t)$:

$$\boldsymbol{f}(x', y', t) = \left(x_0\left(\omega^2 - \lambda^2\right), 0, \left(\omega^2 - \lambda^2\right)\right)^T \tag{9}$$

Since, as previously mentioned, the sign of $\omega^2 - \lambda^2$ is the same as the sign of $|\gamma_2| - 2/\pi$, we draw three conclusions from Eq. (9):

- $\boldsymbol{f}$ and its streamlines are independent of both $\boldsymbol{x}$ and $\boldsymbol{x'}$ coordinates, and of velocity components u and v ($\boldsymbol{f}$ is Galilean invariant); $\boldsymbol{f}(x', y', t)$ depends only on the spatial shift (x_0) between velocity fields $\boldsymbol{u_0}$ and $\boldsymbol{u_1}$ and on $\omega^2 - \lambda^2$.
- A streamline of $\boldsymbol{f}$ seeded at $t = 0$ from any point $\boldsymbol{x'}$ located inside a vortex core ($2/\pi < |\gamma_2| < 1$) evolves in the half-space $t > 0$. On the contrary, if $\boldsymbol{x'}$ is not located inside a vortex core ($|\gamma_2| < 2/\pi$), the streamline is directed towards negative t's.
- The streamlines of $\boldsymbol{f}$ are straight lines inclined with a uniform angle $\tan\alpha = x_0$ relative to the time axis (Fig. 2). Therefore, streamlines relate exactly the original location at t_0 of any point $\boldsymbol{x'}$ inside a vortex core to its new location at t_1.

2.4. Model limitations and application to actual flows

In the previous section, the two main assumptions are that the vortex only experiences a uniform spatial shift between t_0 and t_1, and that velocity gradients are uniform and time-independent in the region where the Taylor expansion is used. Since an actual vortex core is of finite size, parameters λ and ω are in practice not uniform inside the vortex core. Moreover, for a finite time delay $t_1 - t_0$, the vortex core is also subjected to stretching processes and λ and ω are time-dependent. Nevertheless, if velocity fields $\boldsymbol{u_0}$ and $\boldsymbol{u_1}$ are nearly time-resolved, without substantial stretching of the vortex to be tracked, the previous results remain valid in a small region surrounding the center of the vortex core where the Taylor expansion of the velocity field is justified. Therefore, for each vortex identified at t_0 in an actual flow, only one streamline is computed from a single seeding point $\boldsymbol{x'}$ located at the center of the vortex. $\boldsymbol{x'}$ is simply defined as the spatial average of the vortex boundary identified by the condition $|\Gamma_2| = 2/\pi$. Indeed, Γ_2 is preferred to γ_2 used in the theoretical derivations in Section 2.3, since it is a non-local function, less sensitive to measurement noise.

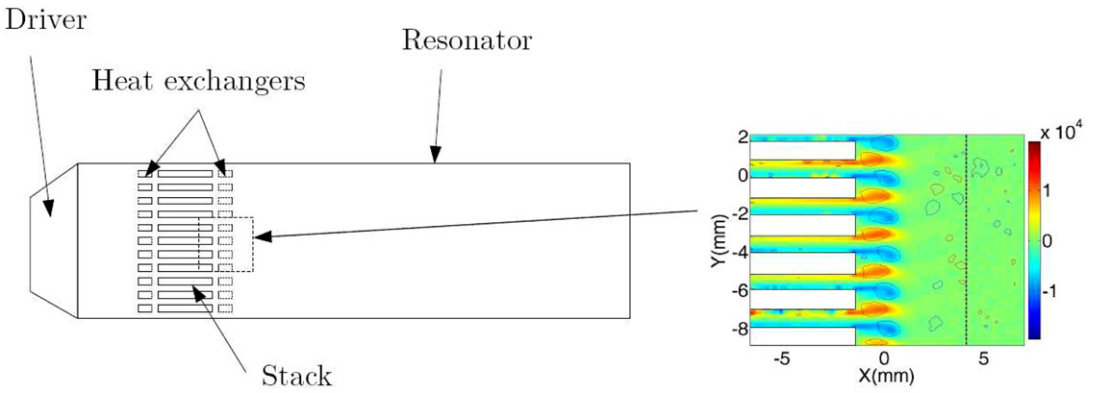

Fig. 3. Schematic drawing of a standing-wave thermoacoustic resonator and example of vorticity field obtained behind the stack. Note that our experimental setup is devoid of heat-exchangers.

3. Application to the study of the flow field behind a stack of parallel plates in an oscillating flow

As an example of the applicability of feature flow field combined with Γ_2 to experimental data, we investigate the flow behind a stack of parallel plates subjected to an acoustic standing wave. Such geometries are common in the domain of thermoacoustic refrigeration, a technology alternative to vapor-compression systems [9]. A schematic drawing of a typical thermoacoustic refrigerator is given in Fig. 3. It consists of a standing-wave acoustic resonator driven by an electro-dynamic loudspeaker. The core of the setup is a stack of plates (hereafter referred to as stack) located adequately inside the resonator. The interaction of the acoustic wave with the solid plates of the stack leads to the pumping of heat from one side of the plates to the other. This heat flux is exploited by heat-exchangers located on both sides of the stack.

Recently, several experimental studies investigated the flow field behind the stack of a thermoacoustic refrigerator using Particle Image Velocimetry (PIV) [10–14]. The latest research efforts focus more particularly on vortex shedding, at high acoustic level, which is expected to affect the efficiency of heat transport from the stack to the heat-exchangers [15,16]. In such flows, a large number of vortical structures is observed because of the spatial periodicity of the stack. A complete description of the flow thus requires an automated procedure for the detection of these vortices and the characterization of their trajectories, which is provided by the joint use of Γ_2 and feature flow field $\boldsymbol{f}$.

The present experimental dataset is extracted from previous measurements that are described in [12]. Measurements focus on the area behind the stack of parallel plates. The plate thickness is 1 mm and the interplate spacing is 1 mm. The amplitude of velocity oscillations is $u_{ac} = 3.6\,\mathrm{m\,s^{-1}}$. Note that PIV measurements are phase-locked with the electrical signal feeding the loudspeaker in order to perform phase-averaging. Results are presented in Fig. 4 for four successive phases of an acoustic period, when the fluid flows out of the stack channels. Each plot represents two-dimensional vorticity fields and isolines of $|\Gamma_2| = 2/\pi$ for a given phase ($t_0 = 0$) and the following one ($t_1 = 1$). Streamlines of $\boldsymbol{f}$ evolve in the three-dimensional (x, y, t) space. Only the flow behind the stack is plotted in Fig. 4, the plates being located at $x < -1$. As the fluid wraps around the edges of the plates, pairs of symmetrical counter-rotating vortices are generated. Vortices are convected away from the stack. Vortices with negative vorticity (in blue) move faster than those with positive vorticity (in red), thus breaking the symmetry of the flow. Eventually, as new vortices are generated, a vortex street appears before all the structures are sucked back into the stack channels when flow reverses (after 180°, see [12]).

Streamlines of $\boldsymbol{f}$ originate at t_0 from seeding points located at the vortex center and are directed towards positive t's. Vortices are convected away from the stack and streamlines of $\boldsymbol{f}$ end at $t = 1$ inside the corresponding vortices that have been shifted between the two phases. Streamlines of $\boldsymbol{f}$ highlight the difference between the convection velocities of vortices with negative (blue streamlines) and positive vorticity (red streamlines). Therefore, it is clear that the flow loses its initial symmetry and evolves into two staggered arrays of counter-rotating vortices. It is also interesting to observe two isolated vortices located at $x > 2$ mm in Fig. 4(a) for a phase equal to 90°. These structures are in fact generated by measurement noise in the velocity field and are not connected to any other vortices at the following phase. Fig. 4(c) shows that a new row of vortices appears at the end of the blowing phase (157.5°) near

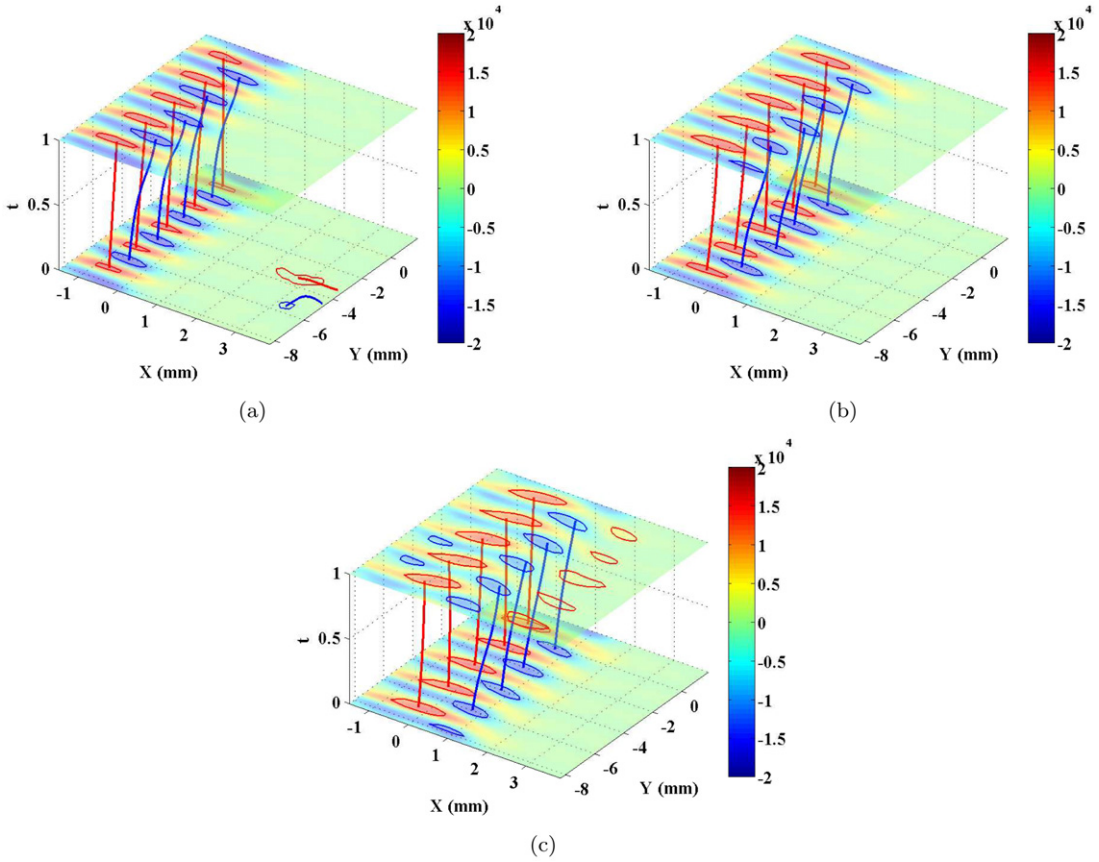

Fig. 4. Streamlines of FFF function linking vortices for two successive vorticity fields behind a stack of plates. For each case, the vorticity field and $|\Gamma_2| < \pi/2$ isolines are drawn for two successive phases, the first phase being in a plane located at $t_0 = 0$ and the second one in a plane at $t_1 = 1$. The streamlines of FFF function evolve between these two planes. (a): from 90° to 112.5°. (b): from 112.5° to 135°. (c): from 135° to 157.5°.

$x = 3$ mm. These vortices do not exist at the previous phase (135°) and are not connected to any streamlines. Hence, measurement noise and vortices that appear only in one snapshot are automatically discriminated by feature flow field. Such results have already been observed by Depardon et al. for the analysis of critical points in a separated flow over a wall-mounted cube. The present results show that the joint use of Γ_2 function and of feature flow field $\boldsymbol{f}$ is a suitable tool for the automated tracking of vortices convected with non-zero velocities.

4. Conclusion

Combining the concept of Feature Flow Field and either functions γ_2 or Γ_2, we have shown that it is theoretically possible to identify and track the location of vortices in a flow, provided that time-resolved velocity data are available and that vortices do not undergo substantial stretching between successive velocity fields. Since $\boldsymbol{f}$ and both functions γ_2 or Γ_2 are Galilean invariant, the tracking of vortices is possible even if they have large convection velocities, which is an improvement compared to the work of Depardon et al. The applicability and interest of the method have been demonstrated for experimental PIV measurements performed in a thermoacoustic refrigerator model. In the future, we intend to study the influence of the combined effects of vortex translation and stretching on the topology of the streamlines of $\boldsymbol{f}$.

Acknowledgements

Part of this work is supported by the French National Research Agency (ANR) under the project MicroThermAc NT051_42101.

References

[1] M.S. Chong, A.E. Perry, B.J. Cantwell, A general classification of three-dimensional flow fields, Phys. Fluids A 2 (1990) 765–777.
[2] J.M. Délery, R. Legendre, H. Werlé, Towards the elucidation of three-dimensional separation, Annu. Rev. Fluid Mech. 33 (2001) 129–154.
[3] S. Depardon, J.J. Lasserre, L.E. Brizzi, J. Boree, Instantaneous skin-friction pattern analysis using automated critical point detection on near-wall PIV data, Meas. Sci. Technol. 17 (7) (2006) 1659–1669.
[4] H. Theisel, H.-P. Seidel, Feature flow fields, in: Data Visualization 2003. Proc. VisSym 03, 2003, pp. 141–148.
[5] L. Graftieaux, M. Michard, N. Grosjean, Combining PIV, POD and vortex identification algorithms for the study of unsteady turbulent, swirling flows, Meas. Sci. Technol. 12 (2001) 1422–1429.
[6] Th. Favelier, M. Michard, N. Grosjean, Développement d'un critère d'identification de structures tourbillonnaires adapté aux mesures de vitesse par PIV, Proc. 9ème Congrès Francophone de Vélocimétrie Laser, E.2.1–E.2.8, Bruxelles, 14–17 Sept. 2004.
[7] J. Jeong, F. Hussain, On the identification of a vortex, J. Fluid Mech. 285 (1995) 69–94.
[8] J.C.R. Hunt, A.A. Wray, P. Moin, Eddies, stream and convergence zones in turbulent flows, Center for Turbulence Research Report CTR-S88, 1988, pp. 193–208.
[9] G.W. Swift, Thermoacoustics: A Unifying Perspective for Some Engines and Refrigerators, Acoustical Society of America, New York, 2002.
[10] Ph. Blanc-Benon, E. Besnoin, O. Knio, Experimental and computational visualization of the flow field in a thermoacoustic stack, C. R. Mecanique 331 (2003) 17–24.
[11] A. Berson, Vers la miniaturisation des réfrigérateurs thermoacoustiques : caractérisation du transport non-linéaire du transport de chaleur et des écoulements secondaires. Thèse de doctorat 2007-41, Ecole Centrale de Lyon, 2007.
[12] A. Berson, M. Michard, Ph. Blanc-Benon, Measurement of acoustic velocity in the stack of a thermoacoustic refrigerator using Particle Image Velocimetry, Heat Mass Transfer 44 (8) (2008) 1015–1023.
[13] D. Marx, H. Bailliet, J.-C. Valière, Analysis of the acoustic flow at an abrupt change in section of an acoustic waveguide using particle image velocimetry and proper orthogonal decomposition, Acta Acustica united with Acustica 94 (2008) 54–65.
[14] P.C.H. Aben, P.R. Bloemen, J.C.H. Zeegers, 2-D PIV measurements of oscillatory flow around parallel plates, Exp. Fluids (2008), available online.
[15] E. Besnoin, O. Knio, Numerical study of thermoacoustic heat exchangers, Acta Acustica united with Acustica 90 (2004) 432–444.
[16] A. Berson, Ph. Blanc-Benon, Nonperiodicity of the flow within the gap of a thermoacoustic couple at high amplitudes, J. Acoust. Soc. Am. 122 (2007) EL122–EL127.